



Title	Prediction of Pulmonary Embolism Following Resection of Pulmonary Infarction : A Case Series
Author(s)	Yamasaki, Hiroshi; Ujiie, Hideki; Kato, Tatsuya; Hida, Yasuhiro; Kaga, Kichizo; Wakasa, Satoru; Matsuno, Yoshihiro
Citation	Annals of Thoracic and Cardiovascular Surgery, 27(6), 371-379 <a href="https://doi.org/10.5761/atcs.0a.20-00396">https://doi.org/10.5761/atcs.0a.20-00396</a>
Issue Date	2021
Doc URL	<a href="http://hdl.handle.net/2115/85065">http://hdl.handle.net/2115/85065</a>
Rights(URL)	<a href="https://creativecommons.org/licenses/by-nc-nd/4.0/">https://creativecommons.org/licenses/by-nc-nd/4.0/</a>
Type	article
File Information	ATCS 27(6) 371-379.pdf



[Instructions for use](#)

**Original  
Article**

# Prediction of Pulmonary Embolism Following Resection of Pulmonary Infarction: A Case Series

Hiroshi Yamasaki, MD,<sup>1</sup> Hideki Ujiie, MD, PhD,<sup>1</sup> Tatsuya Kato, MD, PhD,<sup>1</sup> Yasuhiro Hida, MD, PhD,<sup>1</sup> Kichizo Kaga, MD, PhD,<sup>1</sup> Satoru Wakasa, MD, PhD,<sup>1</sup> and Yoshihiro Matsuno, MD, PhD<sup>2</sup>

**Purpose:** Pulmonary nodules suspected to be cancerous are rarely diagnosed as pulmonary infarction (PI). This study examined the clinical, radiological, and laboratory data in cases diagnosed with PI to determine their potential utility as preoperative diagnostic markers. We also assessed factors affecting the postoperative course.

**Methods:** A total of 603 cases of peripheral pulmonary nodules undiagnosed preoperatively were resected at Hokkaido University Hospital from 2012 to 2019. Of these, we reviewed cases with a postoperative diagnosis of PI. We investigated clinical symptoms, preoperative laboratory data, radiological characteristics, and postoperative complications.

**Results:** Four patients (0.7%) were diagnosed with PI. All patients had a smoking history. One patient received systemic steroid administration, and none had predisposing factors for thrombosis. One case showed chronologically increased nodule size. Three cases showed weak uptake of <sup>18</sup>F-fluorodeoxyglucose. One patient with preoperative high D-dimer levels developed a massive pulmonary embolism (PE) in the postoperative chronic phase and was treated with anticoagulants.

**Conclusions:** Preoperative diagnosis of PI is difficult, and we could not exclude lung cancer. However, if a patient diagnosed with PI has a high D-dimer level, we recommend postoperative physical examination for deep venous thrombosis. Prophylactic anticoagulation therapy should be considered to avoid fatal PE.

**Keywords:** pulmonary infarction, pulmonary embolism, deep venous thrombosis, venous thromboembolism

<sup>1</sup>Department of Cardiovascular and Thoracic Surgery, Hokkaido University Faculty of Medicine and Graduate School of Medicine, Sapporo, Hokkaido, Japan

<sup>2</sup>Department of Surgical Pathology, Hokkaido University Hospital, Sapporo, Hokkaido, Japan

Received: December 28, 2020; Accepted: April 10, 2021

Corresponding author: Tatsuya Kato, MD. Department of Cardiovascular and Thoracic Surgery, Hokkaido University Faculty and School of Medicine, Kita 15 Nishi 7, Kita-ku, Sapporo, Hokkaido 060-8638, Japan

Email: katotatu@huhp.hokudai.ac.jp



This work is licensed under a Creative Commons Attribution-NonCommercial-NoDerivatives International License.

©2021 The Editorial Committee of *Annals of Thoracic and Cardiovascular Surgery*

## Introduction

Recent advances in imaging technology have enabled the identification of small pulmonary nodules in CT screening. Early-stage lung cancer has a favorable prognosis; hence, early surgical intervention is recommended.<sup>1,2)</sup> However, a small and peripheral nodule interferes with the ease of transbronchial lung biopsy and presents difficulty with diagnosis; therefore, determining the timing of surgical interventions can be challenging.<sup>3)</sup> In the present study, we report four cases of pulmonary infarction (PI) diagnosed by postoperative histopathological examination. We experienced one case of massive pulmonary embolism (PE) in the chronic

postoperative phase. Therefore, we investigated whether preoperative laboratory data or radiological features could be used to diagnose PE.

## Materials and Methods

We performed an institutional retrospective analysis of patients undergoing pulmonary resection for a solitary pulmonary nodule or a mass suspicious for lung cancer between January 2012 and December 2019. Patients who had a known diagnosis of benign lesions before resection were excluded from this study. We identified 603 patients who underwent resection of a focal pulmonary lesion in our department of Hokkaido University Hospital. Four of these patients (0.7%) were diagnosed with PE postoperatively and formed the basis of this study. The medical records of each patient were examined for age, sex, body mass index (BMI), smoking history, past medical history, medication, type of surgical resection, laboratory data, echocardiography, chest CT, <sup>18</sup>F-fluorodeoxyglucose positron emission tomography (FDG-PET) results, perioperative complications, and histology. This study was approved by the institutional review board. Before entering the study, the subjects provided informed written consent for their clinical and radiologic data to be used anonymously for the current analysis.

## Results

### Patient background and radiological examinations

Patient characteristics and radiological findings are shown in **Table 1**. The age of these patients ranged from 48 to 74 years (mean 59.3), and all cases were asymptomatic with incidental findings of peripheral lung nodules at chest CT scan for medical checkup or screening for other diseases. Their BMIs ranged from 17.9 to 29.4 (mean 22.5). All patients had a smoking history. Patient 4 received systemic steroid administration for IgG4-related disease and had developed pneumonia twice in the past, but other patients had no particular history that might predispose to thrombosis. Cases 2 and 4 showed complete right bundle branch block (RBBB) on electrocardiogram. Cases 3 and 4 underwent echocardiography for physiologic evaluation but these were normal. Cases 1 and 3 underwent preoperative transbronchial lung biopsy, but we could not confirm the diagnosis. The locations of the nodules varied, but all nodules existed in the subpleural lesion of the peripheral lung and were found by physical examination or screening for other diseases. All nodules

were <20 mm in size. In cases 1, 2, and 4, nodules were round in shape (**Fig. 1A**). Case 3 showed a trabecular shaped nodule in the sagittal section (**Fig. 1B**), and this increased in size at follow-up CT scan 4 months later (**Fig. 1C**). In all cases, the nodules showed spiculation. We performed both plain and enhanced CT in all cases, but there was no enhancement in any of the nodules. In <sup>18</sup>F-FDG-PET scans, cases 1, 3, and 4 showed mild uptake, with the maximum standardized uptake (SUVmax) ranging from 2 to 3, whereas case 2 showed no uptake.

### Laboratory data

Preoperative laboratory data are summarized in **Table 2**. The preoperative D-dimer level was elevated in case 3, but in the other cases, no parameters suggestive of PE were observed. None of the cases showed an inflammatory reaction. Pro-gastrin-releasing peptide was increased in case 3 and neuron-specific enolase in case 1. There were no abnormal findings in the blood gas analysis. Based on these findings, we could not exclude the possibility of lung cancer in any of the cases and decided to perform surgery.

### Surgical procedure and intraoperative findings

In all cases, the operative procedures were thoracoscopic lung wedge resections. Case 1 involved unintended limited resection, because ground-glass opacities (GGOs) were observed in the contralateral lung. In case 3, we did not suspect lung cancer strongly because of the trabecular shape. In cases 2 and 4, we performed wedge resection first, and intraoperative frozen section diagnosis showed no malignant findings. Intraoperative findings in cases 1, 2, and 3 showed pleural indentation, which reflected spicula on CT scan (representative case 3 is shown in **Fig. 2A**). In case 4, the lesion was covered by a pleural plaque.

### Postoperative histopathological findings

In all cases, the nodular, irregular-shaped lesions were located in the subpleural lung parenchyma (**Fig. 2B**). Macroscopically, the cut surface of the lesion was gray-white, scattered with irregular solid areas orange in color, and surrounded by fibrous tissue. Histologically, the lesion was comprised of areas of coagulative necrosis with infiltration of histiocytes and other mononuclear cells. Cholesterol clefts and multinucleated giant cells were also found (**Fig. 2C**). Berlin blue staining showed accumulation of hemosiderin-laden histiocytes, which indicated an ancient intralesional hemorrhage (**Fig. 2D**).

**Table 1 Patient characteristics and radiological appearances**

Case	Age/sex	Symptom	BMI	Smoking (pack years)	Past medical history	Internal medicine	ECG	Cardiac echo	TBLB	Location	Max. size (mm)	Enlargement	Shape	HU (P/E)	SUV max
1	51/M	–	21.7	0.5	25 yo infectious mononucleosis 50 yo dyslipidemia	–	N/A	–	No malignancy	R. S4	20 × 12	–	Round	57/29	2.3
2	48/F	–	29.4	5.5	26 yo cholelithiasis (operation)	–	CRBBB	–	Not performed	R. S6	9 × 7	–	Round	23/-34	None
3	74/M	–	17.9	54.1	6 yo nephrotic syndrome 63 yo hemorrhagic gastric ulcer	–	N/A	N/A	No malignancy	R. S3	17 × 13	+	Trabecular	19/24	3.1
4	64/M	–	21	45	49 yo DM (insulin) 55 yo IgG4-related disease 62 yo, 64 yo pneumonia	Steroid (PSL 10 mg)	CRBBB	N/A	Not performed	L. S1+2	11 × 7	–	Round	60/49	2.6

BMI: body mass index; CRBBB: complete right bundle branch block; DM: diabetes mellitus; ECG: electrocardiogram; F: female; HU: Hounsfield unit; L: left; M: male; Max.: maximum; N/A: not applicable; PSL: prednisolone; R: right; SUVmax: maximum standardized uptake value (of <sup>18</sup>F-Fluorodeoxyglucose-position emission tomography); TBLB: transbronchial lung biopsy; yo: years old

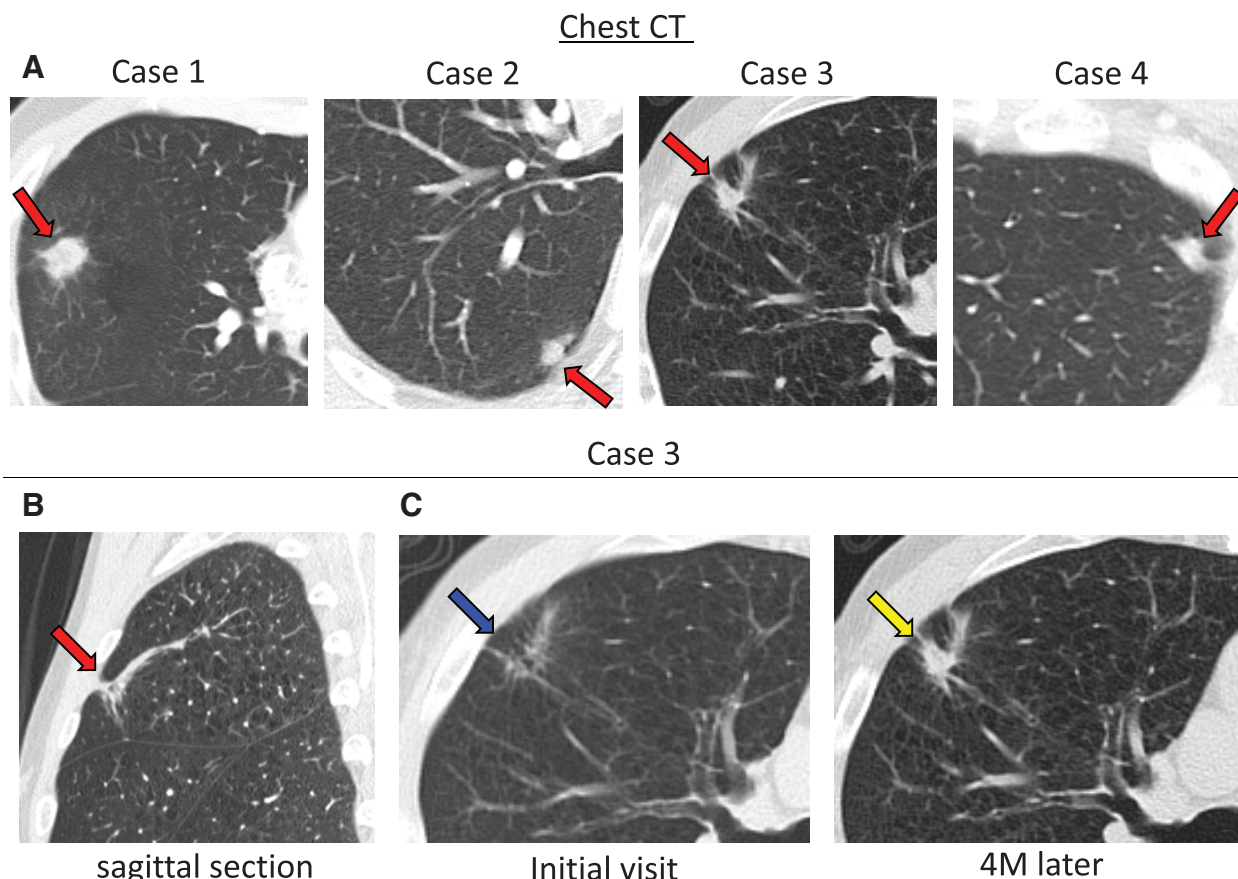


**Fig. 1** (A) Radiographic findings of four cases of pulmonary infarction (PI). CT findings showing all four nodules located in the subpleural lesion of the peripheral lung (red arrows). (B) A trabecular-shaped shadow is seen in a sagittal section of the CT scan in case 3 (red arrow). (C) Axial CT imaging on initial visit (blue arrow). The size of the nodule increased progressively over 4 months (yellow arrow).

Elastica–Masson staining revealed aggregation of alveolar elastic fibers, suggesting focal lung collapse in addition to obstruction of the proximal vessels (Fig. 2E); a diagnosis of distal PI was made, which might have been caused by a locoregional circulatory disorder. Case 3 showed a trabecular shape on CT, but its histopathological findings were not distinguished from the others. Therefore, we did not identify a relationship between the CT and pathological findings.

#### Postoperative course after surgery

All patients had an uneventful postoperative course and were followed-up with no treatment; however, case 3 developed massive PE in the postoperative chronic phase. The detailed information is as follows: 7 months after wedge resection of the right upper lobe, the patient noticed shortness of breath on exercise, which worsened. He saw his home doctor about 1 month after development of symptoms. Echocardiography showed right

heart strain, and an enhanced CT scan showed a large thrombus in the left main pulmonary artery (Fig. 3A); he was considered to need emergency admission to the neighborhood hospital. An enhanced CT scan showed a thrombus in the left femoral vein (Fig. 3B), which was thought to be the origin of the pulmonary embolus.

After initiation of anticoagulation therapy (apixaban 10 mg/day), the thrombus decreased in size and disappeared, and he was discharged 2 weeks later (Fig. 3A). The D-dimer value also decreased after treatment. Since then, he has taken the direct oral anticoagulants (DOAC) apixaban, considering the risk of recurrence. There was no recurrence at 15 months after commencement of the DOAC.

#### Discussion

After encountering a case of massive PE in the postoperative chronic phase following resection of PI



Table 2 Preoperative laboratory data findings

Case	WBC (cells × 10 <sup>9</sup> L)	Neut (%)	RBC (×10 <sup>6</sup> )	Hgb (g/dL)	Hct (%)	Plt (×1000/μL)	PT (s)	APTT (s)	FDP (μg/mL)	Fib (mg/dL)	D-dimer (μg/mL)	CEA (ng/mL)	SCC (ng/mL)	CYFRA (ng/mL)	ProGRP (pg/mL)	NSE (ng/mL)	pCO <sub>2</sub> (mmHg)	pO <sub>2</sub> (mmHg)
1	3.6	55.2	4.77	15.6	45.5	209	12.1	36.6	–	199 L	–	2.3	1	1.2	46.3	12.8 H	46.5 H	93.6
2	4.8	57.1	3.93	11.4 L	34.6 L	408 H	10.8	29.6	<2.6	203	<0.32	0.9 L	N/A	0.6	N/A	N/A	36.5	84.4 L
3	5.6	50.3	4.57	16	45.8	130 L	11.3	26.0 L	3.5	200	1.71 H	3.8	1.6	1.9	87.2 H	10.3	38.7	91.3
4	8.2	71.5	3.82 L	11.7 L	35.5 L	253	9.8 L	30.2	<2.6	230	0.43	2.1	1	3.2	36.8	10	46.2 H	94.4

APTT: activated partial thromboplastin time; CEA: carcinoembryonic antigen; CYFRA: cytokeratin fragment; FDP: fibrin degradation product; Fibg: fibrinogen; Hct: hematocrit; Hgb: hemoglobin; Neut: neutrophil; NSE: neuron specific enolase; pCO<sub>2</sub>: partial pressure of arterial carbon dioxide; Plt: platelet; pO<sub>2</sub>: partial pressure of arterial oxygen; ProGRP: pro-gastrin-releasing peptide; PT: prothrombin time; RBC: red blood cell; SCC: squamous cell carcinoma antigen; WBC: white blood cell

diagnosed postoperatively, we reviewed four cases of PI in our department and examined the clinical, radiological, and laboratory data and their potential utility as preoperative diagnostic markers for PI, as well as assessing factors that affected the postoperative course.

It is known that PI is diagnosed in 8.8%–46.6% of patients with acute PE<sup>4–6</sup>); however, cases of PI with solitary nodules are extremely rare. It appears to occur when microthrombus obstructs the distal portion of small peripheral pulmonary arteries.<sup>7,8</sup> Therefore, the nodule is often located in the subpleural lesion of the lung and is too small to confirm the diagnosis preoperatively.<sup>9</sup> In addition, there are a few reports of PI where cytological examination showed malignancy,<sup>10,11</sup> thus it is difficult to diagnose PI preoperatively.

The characteristic CT findings in cases of PI are of a wedge-shaped or nodular shadow with the pleura as the base, parenchymal density, convex-shaped, bulging borders, and linear strands directed from the apex of the density toward the hilum.<sup>12</sup> However, there are only a few cases that show such typical CT images. Revel et al. reviewed multisection CT images of 50 PIs that did not show direct arterial signs of PE, and 100 peripheral consolidations of other origins; they reported that the presence of central lucencies had 98% specificity and 46% sensitivity for PI.<sup>13</sup> However, the size range of the peripheral consolidations was 2.0–7.8 cm. Our four cases were too small to represent such findings; therefore, these features could not be applied. Thus, there are no clear criteria for radiological findings to diagnose PI in cases with a small and peripheral nodule.

In terms of the past medical histories of our cases, the steroid in case 4 was the only factor that is generally considered to have a risk of PE.<sup>14</sup> On electrocardiogram, cases 2 and 4 showed RBBB, which is also related to PE.<sup>15</sup> However, although RBBB is said to reflect right heart strain, small nodules such as in our cases do not seem to induce strain, unlike in the case of a massive PE. RBBB often occurs in people without PE; thus, the relationship between RBBB and PE has not been confirmed in our study.

Miniati et al. examined 335 patients diagnosed with acute PE by CT and reported that age of approximately 40 years, high body height, low BMI, and current smoking were risk factors for complications of PE and PI.<sup>16</sup> In the present study, all patients had a smoking history, which may be a risk factor for PI. Other laboratory data or patients' past history did not show any clues that made us suspicious of PI but slight increase of D-dimer in case

## Case 3

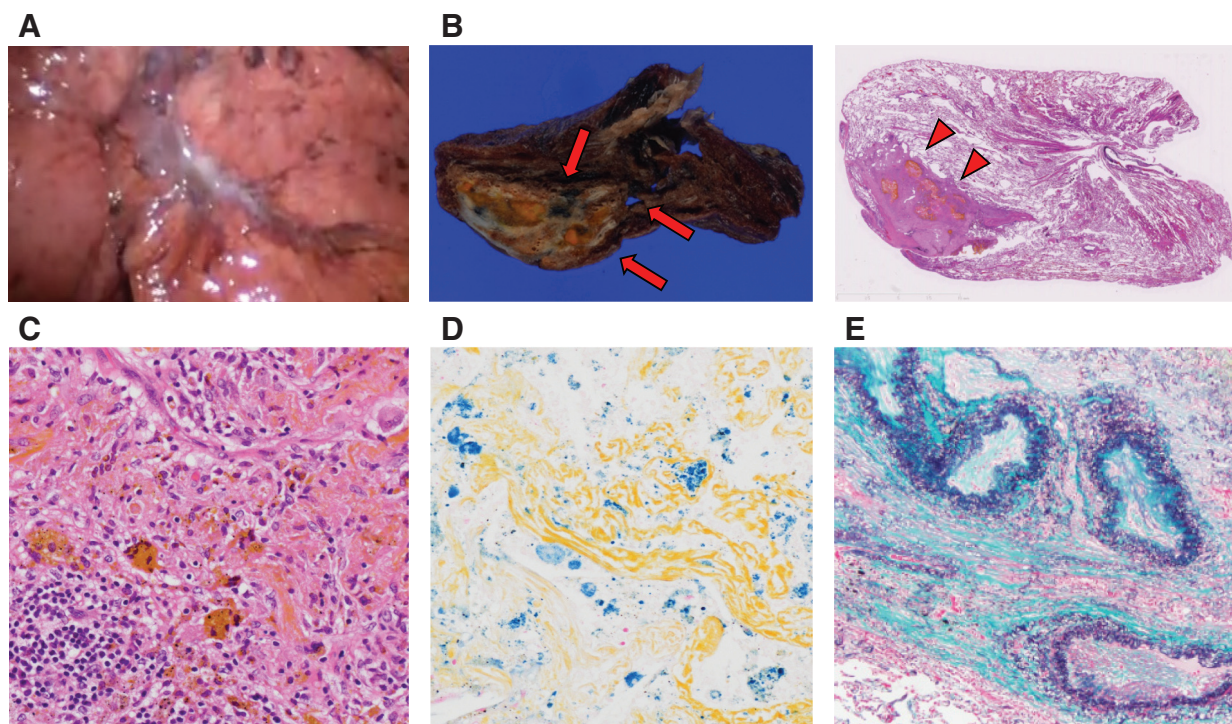


**Fig. 2** Intraoperative and pathological findings of case 3. **(A)** Intraoperative findings showing pleural indentation corresponding to spicula on CT. **(B)** Macroscopic findings. On the cut surface of the resected specimen, scattered irregular orange solid areas are found in the nodule (*red arrows*). A loupe view (hematoxylin and eosin staining) shows nodular, irregular-shaped lesions located in the peripheral and subpleural lung parenchyma (*red arrowheads*). **(C)** Microscopic findings representing necrosis, part of which involves vessels surrounded by fibrosis and the infiltration of histiocytes and other mononuclear cells. The orange-colored region corresponds to hemosiderin-laden histiocytes. **(D)** Berlin blue staining highlights hemosiderin-laden histiocytes. **(E)** Elastica–Masson staining. There is a vascular narrowing and/or occlusion in part of the collapsed lesion.

3. One report documents the disappearance of a pseudo-tumoral PI on repeated CT,<sup>17)</sup> but we encountered a case with a tumor that increased in size over time. Shinohara et al. reported a PI case that showed GGO in the early phase, which reflects the redistribution of the blood flow after obstruction of the pulmonary artery, that subsequently changed into typical CT images.<sup>18)</sup> The radiographic course of case 3, which showed GGO at the initial visit (**Fig. 2B**), was similar to Shinohara et al., suggesting that case 3 was in the early phase of PI at the initial visit. All but one case showed abnormal uptake on FDG-PET. On postoperative histopathological examination, all cases had necrosis in the center of the lesion. Necrotic lesions usually have no uptake on FDG-PET,<sup>19)</sup> but all cases apart from case 2, which showed no uptake, had infiltration of inflammatory cells around the necrotic lesion. Yousem et al. reviewed 23 cases of surgically resected PIs and reported that the area of infarction

showed coagulative necrosis of pulmonary parenchyma associated with extensive areas of hemorrhage in all instances, and in 17 cases (74%), there was a well-defined histiocytic and foamy macrophage margin at the edge of the coagulative necrosis that had a palisaded configuration.<sup>20)</sup> Abnormal uptake seemed to reflect such inflammatory findings.<sup>21)</sup> Soussan et al. reported that PI showed a slight FDG uptake around an area of subpleural consolidation,<sup>22)</sup> which corresponded to histopathological findings.<sup>20)</sup> However, the tumor size of the patients in that study was larger than in ours (median size of the PIs was 48.5 mm [range 30–74 mm]). Our cases, which were smaller than 20 mm, were too small to recognize these findings. Typically, malignant nodules show enhancement on contrast-enhanced CT scans.<sup>23)</sup> We performed both plain and contrast-enhanced CT in all cases and demonstrated no enhancement, suggesting a benign nodule; however, this was insufficient to avoid surgery.

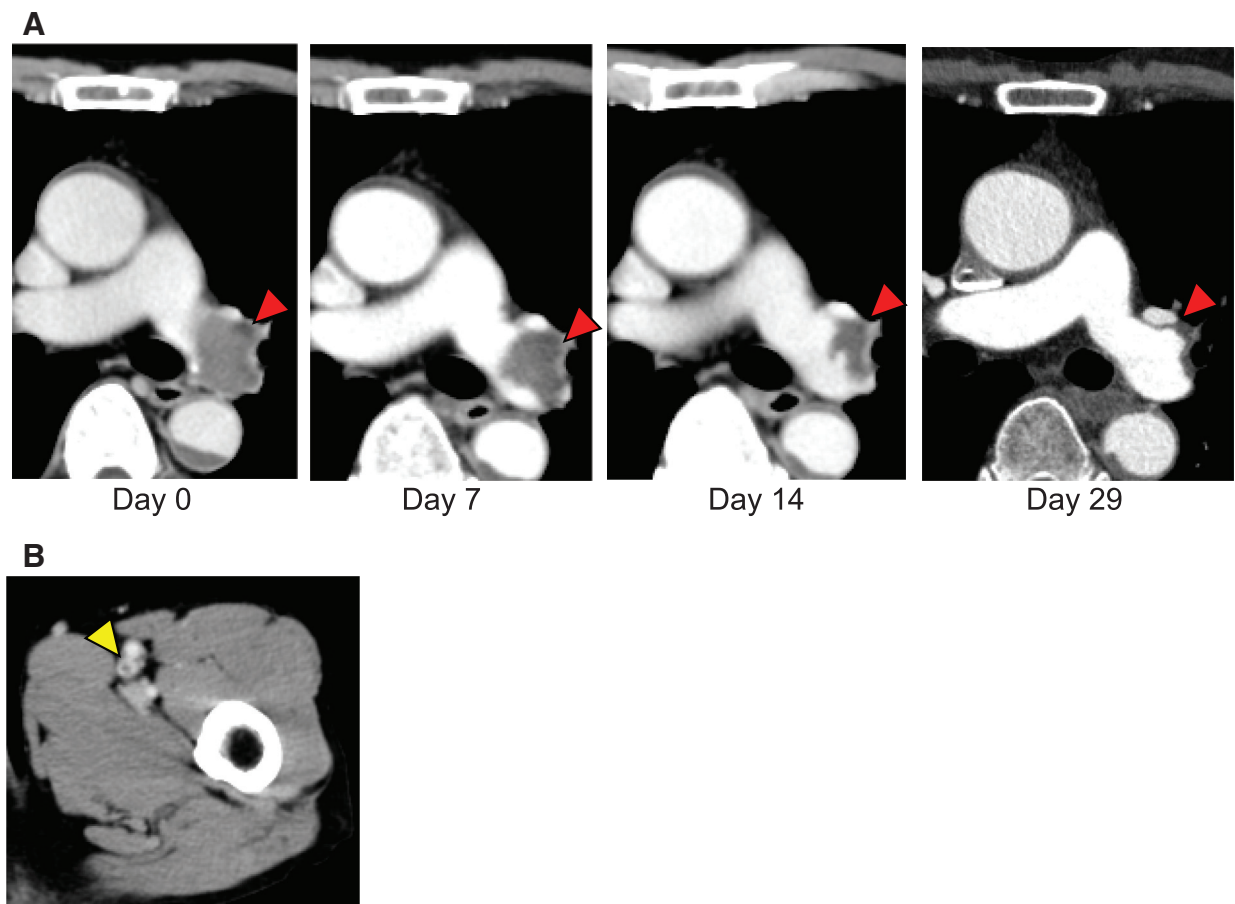


**Fig. 3** Clinical course of case 3. (A) CT scan shows large pulmonary thrombus in the left main pulmonary artery 8 months after surgery. This decreases in size and disappears after starting anticoagulation therapy (red arrowheads). (B) A thrombus is found in the left femoral vein when the diagnosis of pulmonary embolism (PE) is made, and it is considered to be the cause of the PE (yellow arrowhead).

Considering these findings, it is difficult to exclude the possibility of lung cancer preoperatively.

With respect to the causes of PI, Parambil et al. reported a review of 43 PI cases identified by surgical lung biopsy, where the two most common causes were PE (42%) and pulmonary infection (12%).<sup>24)</sup> Infections were diagnosed based on the pathological findings of an intense neutrophilic inflammatory reaction and by identifying an organism through microbial culture of the lung biopsy specimen. In the present series, there was no evidence of infection, and microbial culture did not show any specific findings, but case 4 had developed pneumonia twice in the past, which could be a reason for PI. In terms of PE, which is the most common cause of infarction, although we could not detect an obvious thrombus in the resected specimen, case 3 might be related to PE, considering that the patient developed massive PE 8 months after the operation. PI, with a

peripheral solitary pulmonary nodule, is in itself extremely rare; hence, there are few reports on the development of PE after surgery in this situation. Parambil et al. reported that 2 out of 43 patients who developed PI had recurrent PE. Furthermore, there is a report of patients who underwent surgery for undiagnosed nodules and were diagnosed with PI postoperatively, who died of PE after surgery.<sup>25)</sup> On the basis of this, we should consider the possibility of the development of massive PE in cases of PI with high risk factors.

Case 3 showed a high preoperative D-dimer level. The D-dimer expression level has high sensitivity and negative predictive value for deep venous thrombosis (DVT).<sup>26)</sup> However, our PI cases had almost no D-dimer increase; therefore, D-dimer was not useful for the diagnosis of PI. However, it might indicate the need for a detailed physical examination for DVT and starting anti-coagulants postoperatively.



Eichinger et al. reported that the risk factors for acute PE were age  $\geq 65$  years (44%), obesity with a BMI above 25.3 (34%), long-term bedridden state (23%), cancer (23%), external injury (9%), and thrombus predisposition (6%).<sup>27)</sup> It was also reported that recurrent venous thromboembolism (VTE) was seen in 17.3% of patients with symptomatic PE.<sup>28)</sup> If PI is caused by PE, the recurrence rate of VTE seems to be high. Although we started anticoagulation therapy after the development of the massive PE, we should have conducted a systematic examination for DVT, since it was a PI case, and started postoperative anticoagulants immediately if any thrombus or risk factors were found.

## Conclusion

We should consider a systemic work-up for DVT and commencement of prophylactic anticoagulation therapy when we see a patient with PI with risk factors. In addition, a high D-dimer value in preoperative laboratory data may be helpful for the decision to initiate treatment.

## Disclosure Statement

The authors have no conflicts of interest to declare.

## References

- Howington JA, Blum MG, Chang AC, et al. Treatment of stage I and II non-small cell lung cancer: diagnosis and management of lung cancer, 3rd ed. American College of Chest Physicians evidence-based clinical practice guidelines. *Chest* 2013; **143**: e278S–e313S.
- Sawabata N, Miyaoka E, Asamura H, et al. Japanese lung cancer registry study of 11,663 surgical cases in 2004: demographic and prognosis changes over decade. *J Thorac Oncol* 2011; **6**: 1229–35.
- Rivera MP, Mehta AC, Wahidi MM. Establishing the diagnosis of lung cancer: diagnosis and management of lung cancer, 3rd ed: American College of Chest Physicians evidence-based clinical practice guidelines. *Chest* 2013; **143**: e142S–e165S.
- Cha SI, Shin KM, Lee J, et al. Clinical relevance of pulmonary infarction in patients with pulmonary embolism. *Thromb Res* 2012; **130**: e1–5.
- Islam M, Filopei J, Frank M, et al. Pulmonary infarction secondary to pulmonary embolism: an evolving paradigm. *Respirology* 2018; **23**: 866–72.
- Mançano AD, Rodrigues RS, Barreto MM, et al. Incidence and morphological characteristics of the reversed halo sign in patients with acute pulmonary embolism and pulmonary infarction undergoing computed tomography angiography of the pulmonary arteries. *J Bras Pneumol* 2019; **45**: e20170438.
- Dalen JE, Haffajee CI, Alpert JS, et al. Pulmonary embolism, pulmonary hemorrhage and pulmonary infarction. *N Engl J Med* 1977; **296**: 1431–5.
- Chapman JS. Pulmonary infarction. *South Med J* 1952; **45**: 597–602.
- George CJ, Tazelaar HD, Swensen SJ, et al. Clinicoradiological features of pulmonary infarctions mimicking lung cancer. *Mayo Clin Proc* 2004; **79**: 895–8.
- Lawther RE, Graham ANJ, Mccluggage WG, et al. Pulmonary infarct cytologically mimicking adenocarcinoma of the lung. *Ann Thorac Surg* 2002; **73**: 1964–5.
- Kaminsky DA, Leiman G. False-positive sputum cytology in a case of pulmonary infarction. *Respir Care* 2004; **49**: 186–8.
- Balakrishnan J, Meziane MA, Siegelman SS, et al. Pulmonary infarction: CT appearance with pathologic correlation. *J Comput Assist Tomogr* 1989; **13**: 941–5.
- Revel MP, Triki R, Chatellier G, et al. Is it possible to recognize pulmonary infarction on multisection CT images? *Radiology* 2007; **244**: 875–82.
- Stuijver DJF, Majoor CJ, van Zaane B, et al. Use of oral glucocorticoids and the risk of pulmonary embolism: a population-based case-control study. *Chest* 2013; **143**: 1337–42.
- Hariharan P, Dudzinski DM, Okechukwu I, et al. Association between electrocardiographic findings, right heart strain, and short-term adverse clinical events in patients with acute pulmonary embolism. *Clin Cardiol* 2015; **38**: 236–42.
- Miniati M, Bottai M, Ciccotosto C, et al. Predictors of pulmonary infarction. *Medicine (Baltimore)* 2015; **94**: e1488.
- Lacout A, Marcy PY, El Hajjam M. To avoid operating on pseudo tumoral pulmonary infarctions mimicking lung cancer. *Pan Afr Med J* 2012; **12**: 11.
- Shinohara T, Naruse K, Hamada N, et al. Fan-shaped ground-glass opacity (GGO) as a premonitory sign of pulmonary infarction: a case report. *J Thorac Dis* 2018; **10**: E55–E58.
- Schwarzbach MH, Dimitrakopoulou-Strauss A, Willeke F, et al. Clinical value of [18-F] fluorodeoxyglucose positron emission tomography imaging in soft tissue sarcomas. *Ann Surg* 2000; **231**: 380–6.
- Yousem SA. The surgical pathology of pulmonary infarcts: diagnostic confusion with granulomatous disease, vasculitis, and neoplasia. *Mod Pathol* 2009; **22**: 679–85.
- Kamel EM, McKee TA, Calcagni ML, et al. Occult lung infarction may induce false interpretation of 18F-FDG PET in primary staging of pulmonary malignancies. *Eur J Nucl Med Mol Imaging* 2005; **32**: 641–6.
- Soussan M, Rust E, Pop G, et al. The rim sign: FDG-PET/CT pattern of pulmonary infarction. *Insights Imaging* 2012; **3**: 629–33.

- 23) Swensen SJ, Viggiano RW, Midthun DE, et al. Lung nodule enhancement at CT: multicenter study. *Radiology* 2000; **214**: 73–80.
- 24) Parambil JG, Savci CD, Tazelaar HD, et al. Causes and presenting features of pulmonary infarctions in 43 cases identified by surgical lung biopsy. *Chest* 2005; **127**: 1178–83.
- 25) Miller JI, Harrison EG, Bernatz PE. Surgically treated unsuspected pulmonary infarction. *Ann Thorac Surg* 1972; **14**: 181–8.
- 26) Kelly J, Rudd A, Lewis RR, et al. Plasma D-dimers in the diagnosis of venous thromboembolism. *Arch Intern Med* 2002; **162**: 747–56.
- 27) Eichinger S, Weltermann A, Minar E, et al. Symptomatic pulmonary embolism and the risk of recurrent venous thromboembolism. *Arch Intern Med* 2004; **164**: 92–6.
- 28) Lee S, Jeong H, In K, et al. Clinical characteristics of acute pulmonary thromboembolism in Korea. *Int J Cardiol* 2006; **108**: 84–8.